

Three-Dimensional Mesoporous Chromium Oxide: A Highly Efficient Material for the Elimination of Volatile Organic Compounds**

Anil K. Sinha* and Kenichirou Suzuki

Increasingly strict legislation for controlling the atmospheric emission of industrial volatile organic compounds (VOCs), which contribute to photochemical smog, ground-level ozone, and toxic air emissions,^[1–4] has made the catalytic combustion of hydrocarbons a vital topic of research for the development of new processes for limiting air pollution by VOCs.^[5] Oxides of transition metals such as Mn, Cr, Cu, and Co are the most commonly used, cost-effective catalysts for complete oxidation of VOCs,^[6–9] and crystalline chromium oxide, which favors the formation of CO₂, is the most promising candidate for the total oxidation of organics.^[10]

Ordered mesostructures of transition-metal oxides^[11,12] are of immense interest in areas such as catalysis, sorption, chemical and biological separation, photonic and electronic devices, and drug delivery,^[13] and well-ordered mesoporous oxides of Mn,^[14] Ti,^[15,16] V,^[17] Zr,^[18] W,^[15] Nb,^[15,17] and Ta^[15,18] have been reported. However, the preparation of three-dimensionally (3D) ordered mesoporous oxides of Cu, Co, Cr, Ni, and Fe is more difficult, although it has been possible to prepare unstable lamellar phases of these materials. Recently, hexagonally ordered mesoporous nickel oxide^[19] and wormhole-like mesoporous iron oxide^[20] have been reported. However, nanoporous 3D structure of oxides are more suitable for application as catalysts or adsorbents as they do not suffer from mass-transfer limitations and therefore allow the easier diffusion of reactants.^[21] Transitional-metal oxides are more susceptible to hydrolysis, redox reactions, or phase transitions and possess a number of different coordination numbers and oxidation states, which makes it rather difficult to prepare mesoporous structures from them, unlike silica and aluminosilicates, which can easily form stable mesoporous structures. A neutral templating route has been successfully used for the synthesis of metal-oxide mesostructures^[11,15] that are less readily accessible by electrostatic-templating pathways.^[12,16]

Herein we demonstrate for the first time that a 3D mesoporous chromium oxide material, prepared by a neutral templating route, shows an exceptionally high removal/

oxidation ability for VOCs (toluene, acetaldehyde) after calcination. For transition-metal oxides, control of the rates of precursor hydrolysis, condensation of metal species, and precipitation of mesostructured oxides, for example by slow crystallization, is an important prerequisite for the enhanced framework cross-linking^[22,23] that leads to a stable mesoporous structure. We therefore used a metal nitrate salt precursor, a mixed nonaqueous, ethylene glycol/propanol medium, and poly(alkylene oxide) block copolymers as template to prepare a very stable 3D mesoporous structure. The mixed nonaqueous medium allows a very slow crystallization (gelation) process, which favors the formation of a stable mesostructure by enhanced framework cross-linking. Our intention was to exploit such a material with 3D mesoporosity, large surface area, high oxidizing power, and probable ready evolution of active lattice oxygen, to prepare a commercially viable, cost-effective catalyst/sorbent system for the efficient removal of VOCs at low temperatures.

The as-synthesized mesoporous chromium oxide samples were transparent, and formed a fluffy, foamlike material after heating in air at 150 °C. Thermogravimetric experiments indicated that the template molecules could be completely removed by calcinating the samples at 400 °C; this was confirmed by C,H analysis.

Typical X-ray diffraction (XRD) patterns for the mesostructured chromium oxide before and after organic-template removal are shown in Figure 1a. The as-made chromium

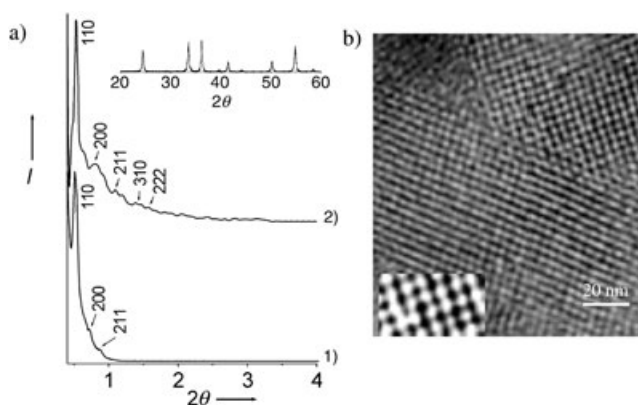


Figure 1. a) XRD pattern of mesoporous chromium oxide: 1) as-made and 2) template-free (heated to 150 °C and extracted with ethanol); b) TEM image of the template-free mesoporous chromium oxide. Inset: the reconstructed image of a selected region.

inorganic/polymer mesostructure shows diffraction peaks with lattice spacings, *d*, of 173, 122, and 100 Å. The *d*-value ratios for these peaks are $\sqrt{2}:\sqrt{4}:\sqrt{6}$, and they are indexable as (110), (200), and (211) reflections, respectively, in the cubic *Im3m* space group. Five major XRD peaks, with *d* spacings of 150, 106, 87, 67, and 61 Å and *d*-value ratios $\sqrt{2}:\sqrt{4}:\sqrt{6}:\sqrt{10}:\sqrt{12}$, are observed after removal of the organic block-copolymer template. They are similarly indexable as the (110), (200), (211), (310), and (222) reflections of the cubic *Im3m* space group. The basal spacing is observed to decrease by 23 Å upon removal of the template due to lattice contraction. The wide-angle X-ray diffraction pattern of the

[*] Dr. A. K. Sinha, K. Suzuki
Toyota Central R&D Labs Inc.
41-1, Aza, Yokomichi, Nagakute-cho
Aichi-gun, Aichi-ken 480-1192 (Japan)
Fax: (+81) 561-63-6137
E-mail: sinha-anil@mosk.tytlabs.co.jp

[**] We thank Mr. N. Suzuki and Ms. N. Takahashi of Toyota CRDL Inc. for transmission electron microscopy (TEM) and X-ray photoelectron spectroscopy (XPS) analyses, respectively.

Supporting information for this article is available on the WWW under <http://www.angewandte.org> or from the author.

template-free calcined sample (Figure 1a, inset) clearly shows peaks that can be indexed according to the rhombohedral phase of crystalline Cr_2O_3 , thus indicating the presence of trivalent Cr in the sample. However, the presence of other mixed-valent Cr species cannot be ruled out because X-ray photoelectron spectroscopy (XPS; vide infra) revealed the presence of Cr species with different oxidation states.

The XRD peak assignment was further confirmed by transmission electron microscopy (TEM). The TEM image of the mesopore arrangement is shown in Figure 1b, where a regular arrangement of bright spots and ordered channels is observed that is attributed to the three-dimensional cubic ordered arrangement of mesopores.

The N_2 adsorption–desorption isotherm and Barret–Joyner–Halenda (BJH) pore-size distribution for the 3D mesoporous chromium oxide are presented in Figure 2. The

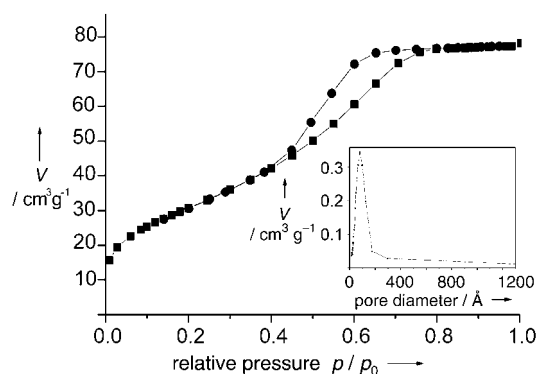


Figure 2. N_2 sorption isotherm and pore-size analysis (inset) of the mesoporous chromium oxide calcined at 400 °C.

sample exhibits a type-IV isotherm that is typical of mesoporous materials, with a well-defined step in the adsorption curve between partial pressures, p/p_0 , of 0.4 to 0.8, and a large hysteresis loop due to capillary condensation in the mesoporous channels and/or cages. BJH analysis of the adsorption data, assuming cylindrical pores, shows that the calcined mesoporous chromium oxide has a mean pore-size of 7.9 nm and a wall thickness of 13.3 nm, as estimated from the XRD unit-cell parameter (a_0) value of 21.2 nm. The absence of textural mesoporosity is indicated by a plateau at a relative pressure of about 0.8 to 1.0. The template-free sample (after ethanol extraction) has a surface area of $212 \text{ m}^2 \text{ g}^{-1}$, which decreases to $96 \text{ m}^2 \text{ g}^{-1}$ after calcination at 400 °C and to $78 \text{ m}^2 \text{ g}^{-1}$ after calcination at 500 °C.

A sample (0.4 g) of the 3D mesoporous chromium oxide calcined at 500 °C showed the highest toluene removal ability among all these materials, with 52% toluene removal and 11 ppm CO_2 formation (2% conversion) after 25 h at room temperature (sample 3 in Figure 3). The toluene-removal ability increased to 65%, with 66 ppm CO_2 formation (12% conversion), when the temperature was increased to 85 °C (sample 4). An increase in toluene-removal ability with increasing temperature is an indication of catalytic oxidation of toluene at low temperatures. This is the first report of partial catalytic decomposition of VOCs by mesoporous transition-metal oxides at low temperature. In comparison,

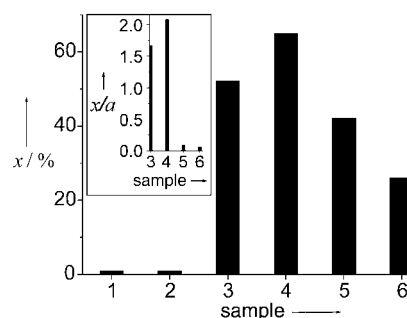


Figure 3. Toluene removal (x) over various chromium oxide samples: 1) commercial Cr_2O_3 , 2) commercial CrO_3 , 3) mesoporous CrO_x (at room temperature), 4) mesoporous CrO_x (at 85 °C), 5) mesoporous SiO_2 (room temperature), 6) mesoporous SiO_2 (at 85 °C). The inset shows the toluene removal per unit area of the samples (x/a).

mesoporous silica with a surface area of $1120 \text{ m}^2 \text{ g}^{-1}$ showed 42% toluene removal at room temperature (sample 5), which decreased to 26% when the reaction temperature was increased to 85 °C (sample 6). Even though the 3D mesoporous chromium oxide has a surface area about 10 times lower than that of mesoporous silica, it still shows a much higher toluene-removal ability. The toluene-removal ability per unit area is about 18 times higher at room temperature, and about 35 times higher at 85 °C, for mesoporous chromium oxide than for mesoporous silica (Figure 3, inset). It was possible to achieve 94% toluene removal with 1.0 g of 3D mesoporous chromium oxide (see Supporting Information). Commercial hexavalent and trivalent chromium oxide (Wako Chemicals) samples (samples 1 and 2) gave less than 1% toluene removal. A high-surface-area amorphous chromia aerogel ($278 \text{ m}^2 \text{ g}^{-1}$),^[24] which contains mostly trivalent chromium species (from XPS analysis), also showed a low toluene-removal performance (<10%).

The X-ray photoelectron spectrum of the mesoporous chromium oxide sample shows a broad band, which indicates the presence of Cr in multiple oxidation states from +2 to +6 (see Supporting Information) with about 75% of the Cr present in the +3, or lower, oxidation state. This implies that the mixed oxidation state of the 3D mesoporous chromium oxide sample, as well as its high surface area and 3D mesoporosity, is probably responsible for the exceptionally high toluene-removal ability. Strong π -d^[25] and d- σ interactions,^[26] the possibility of ready evolution of active lattice oxygen species, as well as the high oxidizing power of higher valent Cr species favored by lattice strain, is probably responsible for the excellent toluene-removal ability of this mesoporous chromium oxide. In fact, when the toluene combustion reaction was evaluated in a flow reactor the toluene decomposition was found to start well below 100 °C, and it was possible to achieve 100% toluene combustion at temperatures of 280–300 °C (see Supporting Information).

These 3D mesoporous oxides could therefore be excellent materials for the sorption of VOCs at room temperature. The adsorbed VOCs can then be directly decomposed by the same catalyst at higher temperatures, thereby eliminating the need for the elimination of VOCs from the sorbent as is required for conventional VOC-removal materials such as activated

carbon or porous silica. We were able to completely decompose the toluene adsorbed on the surface of the catalyst by thermal treatment at around 350 °C, and the regenerated catalyst could be reused without any loss in activity. XPS analysis did not show any change in the oxidation state of Cr after regenerating the 3D mesoporous oxide. There was also little change in the surface area of the regenerated catalysts. Further work on the long-term use of these catalysts is still underway to determine the total catalyst lifetime and coking behavior.

The 3D mesoporous chromium oxide catalyst (0.4 g) also removed 94 % of the acetaldehyde from a 27 ppm acetaldehyde feed in air after reaction at room temperature for 25 h.

In summary, we have reported a commercially viable 3D mesoporous chromium oxide sorbent/catalyst with an exceptionally high VOC elimination ability. We expect to be able to develop a novel, dual-function sorbent/catalyst material—under ambient conditions the material acts as a selective sorbent for the VOCs, then, when it is heated to higher temperature, it acts as an effective and selective deep-oxidation catalyst for the VOCs so that the recovery and/or incineration step required in the case of currently available commercial VOC adsorbents can be eliminated. These mesoporous oxides also have potential applications as catalysts for various organic transformations, as supports, adsorbents, and separation materials, and in sensors, porous electrodes or electrolytes, and electromagnetic and electronic devices.

Experimental Section

Triblock copolymer F-127 ($\text{HO}(\text{CH}_2\text{CH}_2\text{O})_{106}(\text{CH}_2\text{CH}(\text{CH}_3)\text{O})_{70}(\text{CH}_2\text{CH}_2\text{O})_{106}\text{H}$) and chromium nitrate were used as the template and inorganic source, respectively. The typical molar gel composition was 134 Cr:1115 propanol:1080 EG:1 F-127 (or P-123). In a typical synthesis, F-127 block copolymer (1 g) was dissolved in a mixture of propanol (5 g) and ethylene glycol (EG; 5 g). $\text{Cr}(\text{NO}_3)_3 \cdot 3\text{H}_2\text{O}$ (2.42 g) was added to this solution with vigorous stirring over 30–40 min. The resulting sol solution was then aged at 40–50 °C for 7–14 days and then heated gradually (1 °C min⁻¹) to 150 °C. Finally, the organic template molecules were removed by extracting with ethanol. The samples were further calcined by heating gradually (1 °C min⁻¹) to 300–500 °C.

A gas mixture containing 103.3 ppm toluene, 20 % oxygen, and the balance as nitrogen was used as the evaluation gas. A 0.4-g sample of each of the aforementioned catalysts and the evaluation gas were put in a 5-L gas container. The gas was analyzed after different time intervals by GC (Shimadzu, column Sp-1000) and a CO₂ analyzer (LI-6262, LI-COR, Inc.). The toluene conversion was determined from the equation: toluene removal (%) = $\frac{[(\text{toluene concentration in gas container without catalyst}) - (\text{toluene concentration in gas container with catalyst})]}{(\text{toluene concentration in gas container without catalyst})} \times 100$.

A packed-bed reactor was used to evaluate the catalysts' activity in the complete oxidation of toluene (space velocity 30000 h⁻¹; toluene: 100 ppm; oxygen: 18 %; and the balance of nitrogen). At the onset of the reaction the catalyst was pretreated with reactant mixture at 180 °C for 1.5 h to prevent over-estimation of toluene conversion caused by adsorption of toluene during the initial stages of the test.

Keywords: adsorption · chromium · environmental chemistry · mesoporous materials · oxidation

- [1] J. J. Spivey, *Ind. Eng. Chem. Res.* **1987**, 26, 2165.
- [2] W. Chu, H. Windawi, *Chem. Eng. Prog.* **1996**, 92, 37.
- [3] B. K. Hodnett, *Heterogeneous Catalytic Oxidation, Fundamentals and Technological Aspects of the Selective and Total Oxidation of Organic Compounds*, Wiley, Chichester, **2000**, p. 191.
- [4] G. Centi, P. Ciambelli, S. Perathoner, P. Russo, *Catal. Today* **2002**, 75, 3.
- [5] M. F. M. Zwinkels, S. G. Jaras, P. G. Menon, *Catal. Rev. Sci. Eng.* **1993**, 35, 319.
- [6] D.-C. Kim, S.-K. Ihm, *Environ. Sci. Technol.* **2001**, 35, 222.
- [7] Y. Moro-oka, A. Ozaki, *J. Catal.* **1966**, 5, 116.
- [8] D. L. Trimm, *Appl. Catal.* **1983**, 7, 249.
- [9] *Catalytic Control of Air Pollution* (Eds.: R. G. Silver, J. E. Sawyer, J. C. Summers), American Chemical Society, Washington DC, **1992**.
- [10] C. M. Pradier, F. Rodrigues, P. Marcus, M. V. Landau, M. L. Kaliya, A. Gutman, M. Herskowitz, *Appl. Catal. B* **2000**, 27, 23; H. Rotter, M. V. Landau, M. Carrera, D. Goldfarb, M. Herskowitz, *Appl. Catal. B* **2004**, 47, 111.
- [11] P. Yang, D. Zhao, D. I. Margolese, B. F. Chmelka, G. D. Stucky, *Nature* **1998**, 396, 152.
- [12] F. Schüth, *Chem. Mater.* **2001**, 13, 3184.
- [13] X. He, D. Antonelli, *Angew. Chem.* **2002**, 114, 222; *Angew. Chem. Int. Ed.* **2002**, 41, 214.
- [14] Z.-R. Tian, W. Tong, J.-Y. Wang, N.-G. Duan, V. V. Krishnan, S. L. Suib, *Science* **1997**, 276, 926.
- [15] P. Yang, D. Zhao, D. I. Margolese, B. F. Chmelka, G. D. Stucky, *Chem. Mater.* **1999**, 11, 2813.
- [16] D. M. Antonelli, J. Y. Ying, *Angew. Chem.* **1995**, 107, 2202; *Angew. Chem. Int. Ed. Engl.* **1995**, 34, 2014.
- [17] P. Liu, I. L. Moudrakovski, J. Liu, A. Sayari, *Chem. Mater.* **1997**, 9, 2513.
- [18] D. M. Antonelli, J. Y. Ying, *Chem. Mater.* **1996**, 8, 874.
- [19] S. Banerjee, A. Santhanam, A. Dhathathreyan, P. M. Rao, *Langmuir* **2003**, 19, 5522.
- [20] D. N. Srivastava, N. Perkas, A. Gedanken, I. Felner, *J. Phys. Chem. B* **2002**, 106, 1878.
- [21] A. K. Sinha, S. Seelan, S. Tsubota, M. Haruta, *Angew. Chem.* **2004**, 116, 1572; *Angew. Chem. Int. Ed.* **2004**, 43, 1546.
- [22] J. Livage, M. Henry, C. Sanchez, *Prog. Solid State Chem.* **1988**, 18, 259.
- [23] C. F. Baes, Jr., R. E. Mesmer, *The Hydrolysis of Cations*, Wiley, New York, **1976**.
- [24] M. Abecassis-Wolfovich, H. Rotter, M. V. Landau, E. Korin, A. I. Erenburg, D. Mogilyansky, E. Gartsstein, *J. Non-Cryst. Solids* **2003**, 318, 95.
- [25] A. A. Davydov, *Infrared Spectroscopy of Adsorbed Species on the Surface of Transition Metal Oxides*, Wiley, New York, **1990**, p. 195; A. A. Davydov, V. G. Mikhaltchenko, V. D. Sokolovskii, G. K. Borekov, *J. Catal.* **1978**, 55, 299.
- [26] M. R. Albert, J. T. Yates, *The Surface Scientist's Guide to Organometallic Chemistry*, American Chemical Society, Washington DC, **1987**.

Received: July 13, 2004